Misan Journal of Engineering Sciences ISSN-E: 2957-4250
Vol. 1, No. 1, June 2022 ISSN: 2957-4242

Improving RC Beam-Column Joints Characteristics Using Different Reinforcement Details

Dhiaa Chasib Resheq[1] and Abdulkhaliq A. Jaafer[2*]

[1]*Missan Oil Company, Maysan, Iraq*
[2]*Department of Civil Engineering, College of Engineering, University of Misan, Maysan, Iraq*
**Corresponding author E-mail: aljabery@uomisan.edu.iq*

(Received 27 Jan , Revised 23 Mar , Accepted 20 May)

Abstract: This paper aims to study the effect of concrete confining using a new style of internal closed stirrups and longitudinal steel bars along with the middle third of the beam length of the beam-column joints. Also, the influence of concrete compressive strength was investigated using three types of concrete normal strength concrete (NSC), high strength concrete (HSC), and steel fiber concrete (SFRC). Nine reinforced concrete specimens with the same dimensions are divided into three groups according to the concrete type with different reinforcement details in the middle third of the specimen's length. Four specimens with (NSC) represent the first group, while three specimens consist in the second group with (HSC). Steel fiber of 2% was used in two specimens of the third group (SFRC). The test results showed that using additional reinforcement steel bars as a closed stirrup arranged about the neutral axis improved the flexural strength and enhanced the load-carrying capacity for the reinforced concrete joints. The ultimate capacity of the joints increased by a range (34 to 50) % more than the control specimen. The ultimate strength was also increased for the specimens due to using high-strength concrete with a range (of 13 to 66) % compared with the specimen of normal compressive strength.

Keywords: beam-column joint; monotonic load; steel fiber; concrete compressive

1. Introduction

The performance of beam-column joints has long been recognized as a significant factor that frequently becomes critical for the overall behavior of reinforced concrete (RC) framed structures subjected to seismic loads[1] Many studies have been achieved to improve the ductility characteristics of the joint or to change the failure mode by changing a plastic hinges location. Ha and Cho presented a study that aimed to change the plastic hinge location at the beam-column joint away from the face of a column by providing a special anchorage for confining concrete[2]. [3] studied non-seismic reinforced concrete joint strengthened using carbon fiber reinforced polymer to enhance the lateral strength and ductility. [4] explained the ability of beam-column joints strengthened by GFRP bars and stirrups subjected to simulated seismic load conditions to bear a 4% drift ratio without any respectable residual deformation and showed that increasing the reinforcement ratio of the joint supports the understanding of the strong column-weak beam concept. A new strengthening technique for RC joint using sheet and corner block pre-manufactured and fixed at the joint with anchor rod was achieved[5]. [6] investigated the ferrocement Jacketing is a strengthening technique for exterior RC joints using conventional and advanced jacketing. A new strengthening technic on exterior non seismically reinforced concrete beam-column joint by using both CFRP and the circular concrete cover was carried out by Hadi and Tran. The share capacity of the strengthening joint is quite enhanced[7]. [8] experimentally proved using engineered cementitious composite with polypropylene fiber and hybrid cementitious composites derived from increasing the load capacity, shear capacity and damage tolerance capacity, and member ductility. [9] investigated the improvement of the seismic capacity for exterior beam-column joints using concrete jacketing. The obtained results showed that using concrete jacketing changed the failure mode to be flexural instead of shear failure. [10] Different kinds of RC joints were studied, such as exterior, interior, T, and knee joints. Various parameters were included in these studies, such as the compressive strength of concrete and longitudinal and transverse reinforcement. [11] Studied the behavior of exterior reinforces

concrete beam-column joint that SIFCON improved. They concluded that both SIFCON joints and specimen with SIFCON in the joint core exhibited a good ductile behavior under the applied load before the final collapse. Using stiffened steel plates, they relocated the plastic hinge location and increased the joint capacity for retrofitted specimens[12] This technique enhanced the seismic performance of the joint by moving the plastic hinge location out of the renovated area. The weak beam- strong column strategy to improve beam-column joint was adopted by[13] The study proved that the sudden failure of a joint could be avoided by using diagonal steel bars. [14] Investigated the efficiency of exterior retrofitted RC beam-column joint using GFRP as externally bonded sheets and NSM strips in different angles (30,45 and 60) of GFRP. The study proved that the NSM technique with an angle of 30 degrees proves the stiffness, ductility, energy dissipation, and strength. [15] investigated the behavior of RC beam-column joint using three types of different fibers (carbon, glass, and steel). Concerning ductility and strength, the results improved [16] studied the effect of using steel sections to improve the ductility characteristics of the RC beam-column joint (T-shape). The ductility was significantly enhanced when compared with the result with the conventional one. [17] studied the relocation of plastic hinge location for strengthened RC beam-column joint using carbon fiber reinforced polymer. The results showed that the plastic hinge location moved to the end of the CFRP sheet, and the required length of the bonded CFRP sheet should be lesser than that of the beam depth. [18,19] investigated the effectiveness of steel fiber vary (0.75 to 1.5) % on the whole behavior of RC beam-column joints. All the studied fibrous concrete specimens showed almost similar lateral strength, dissipation of the energy, and defeat style even without a transverse steel joint core. Due to the lack of information from the previous studies concerning confining the RC joint using special details of reinforcement, the main objective of this study is to investigate the effect of additional interior steel reinforcement with different details on the carrying capacity of the RC joint. Also, the effect of the concrete compressive strength on the joint performance represents the other goal. Three types of concrete which are normal concrete, high strength, and ultra-high-strength concrete, are selected in this study. To perform the purposes of the study, nine RC joints are tested.

2. Experimental Program

2.1 Materials

Various materials have been used to produce three types of concrete (Normal Strength concrete NSC, High Strength Concrete HSC, and Steel Fiber Reinforced Concrete SFRC) used for casting the specimens. Ordinary Portland cement, fine aggregate, coarse aggregate with a maximum size of 10 mm, silica fume, straight steel fiber 14 mm length with aspect ratio 70, reinforcement steel bars Ø (10 and 6) potable clean water superplasticizer hyperplastic PC260 were used.

2.1.1 Reinforcement Steel Bars.

Deformed steel bars were used to a reinforcement of the specimens. Reinforcing steel bars of Ø10 mm was used as the main reinforcement in beam and column, while steel bar of Ø6 mm was used for stirrups in beam and ties in a column. Table 1 shows the properties of used reinforcement steel.

Table 1 Properties of reinforcement steel bars.

Nominal diameter (mm)	Actual diameter (mm)	Yield stress (fy) (MPa)	Ultimate stress (fu) (MPa)	Elongation %
6.00	5.97	442.62	503.60	11.10
10.00	9.46	560.60	652.50	12.40

2.1.2 Concrete.

Three types of concrete were used for casting the specimens. Table 2 shows the details of these types of concrete and the weight of materials used per cubic meter.

Table 2 Details of used concrete types.

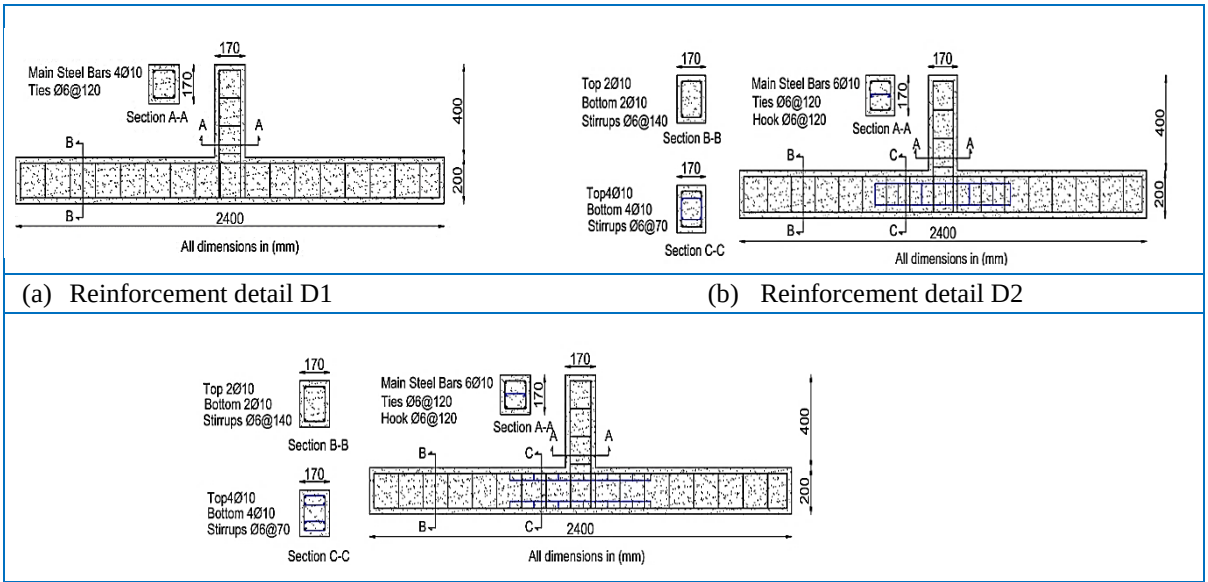
	Concrete Type		
	NSC	HSC	SFRC
F_{cu} (MPa)	43	83	122
Cement (kg/m3)	450	500	950
Fine aggregate (kg/m3)	562	625	1050
Coarse Aggregate (kg/m3)	675	750	-
Silica fume (kg/m3)	-	50	209
Water (L/m3)	225	125	220
Steel Fiber (kg/m3)	-	-	156
Hyperplast PC260 (kg/m3)	-	11	34.77

2.2 Specimens Details

Nine RC beam-column joint specimens have been cast with the same dimensions. Three reinforcement details and three types of concrete were adopted for producing the specimens. Table 3 shows the details of the specimens, while Fig.2 shows the reinforcement details.

Table 3 Specimens details

Group	Type	designation	Description	Reinforce-ment
A	NSC	C1	Control 1	D1
		C2	Control 2	
		N1D2		D2
		N2D3		D3
B	HSC	H1D1	Control	D1
		H2D2		D2
		H3D3		D3
C	SFRC	F1D1	Control	D1
		F2D2		D2



(a) Reinforcement detail D1

(b) Reinforcement detail D2

(c) Reinforcement detail D3

Fig.2 Reinforcement details

2.3 Test Set-Up

The test was carried out on RC beam-column joint specimens at the Structural Materials Laboratory of the Technical Institute in Misan province. UTEST flexural frame test (600 kN) capacity was used for testing the specimens. All the RC specimens were tested up to failure under monotonic load as inverted T-section. The load was applied vertically downward to the face of the column (one-point load) and manually increased up to failure. The mid-span deflection was obtained by installing a dial gauge under the specimens. Fig. 3 shows the testing machine and test setup.



Fig. 3 Testing machine and specimen test set-up

3. Test Results and Discussion

Under this item, two parameters will be discussed, the effect of confining concrete by internal closed stirrups and concrete compressive strength on the load-carrying capacity, ductility index, toughness, initial stiffness, and failure mode of tested specimens. After the collapse of all specimens, all the failure characteristics were briefed in Table4. To show the development of the ductility characteristics of the joint due to change of reinforcement detail, specimens of each group will be compared to their control specimen, while to explain the effect of compressive strength, the comparison will be among the three groups specimens that have same reinforcement details.

3.1 Load – Carrying capacity

From the results of the ultimate load that showed in Table 4, all specimens of concrete confining using internal closed stirrups showed an increase in their carrying capacity. For group "A" with normal concrete specimens, the ultimate load for the specimens reinforced as details D2 and D3 showed an increase ranging (from 48 and 50) % respectively, compared to the average loads of the specimens with conventional reinforcement detail D1. The ultimate load of high-strength concrete specimens of group "B" was enhanced by (44 and 47) % for the specimens of reinforcement detail D2 and D3, respectively, compared to their reference specimen. Also, the ultimate load of steel fiber reinforced concrete specimens of group "C" was increased due to using reinforcement detail D2 by 34% compared to the specimen of normal reinforcement detail. It is worth noting that using internal details D2 and D3 enhanced the load-carrying capacity for the specimens almost equally due to the arrangement of the additional longitudinal steel bars and internal closed stirrups around the beam's neutral axis. The increase in final load capacity resulted from the increase in the tensile strength of the concrete due to using additional reinforcement steel, i.e. (D2 and D3). Also, the confinement of concrete helps to restrain cracks, delay the cracks' appearance, and prevent their extension.

Furthermore, when the concrete compressive strength increased, the high-strength concrete and steel fiber reinforced concrete was used, and the ultimate load carrying capacity for the specimens increased too. For reinforcement detail, D1, the increase of the maximum loads that were sustained by high strength and steel fiber concrete specimens are (16 and 66) % compared to the normal concrete specimens with the same reinforcement detail. An increase of (13 and 51) % for the specimens of HSC and SFRC with reinforcement detail D2, respectively, compared to the specimen of NSC. The increase achieved by the specimen of HSC with reinforcement details D3 was 13% compared to a normal concrete specimen with the same steel detail; when the concrete compressive strength increased, the

flexural strength and shear strength increased, too, which derived from increasing the carrying load.

Table 4 Failure characteristics of all beams after the collapse

Group	Designation	Reinforcement detail	Maximum load (kN)	First crack load (kN)	Mid-span deflection (mm)	Toughness (kN.mm)	Ductility index	Initial Stiffness (kN/mm)
A	C1	D1	34.20	13.60	23.80	626	2.80	3.32
	C2	D1	32.70	12.90	23.45	590	2.67	3.30
	N1D2	D2	49.40	20.10	27.48	1005	3.16	3.67
	N2D3	D3	50.30	22.20	28.50	1120	3.35	3.99
B	H1D1	D1	38.80	18.20	27.95	863	5.27	3.82
	H2D2	D2	55.90	24.20	28.47	1173	6.70	4.31
	H3D3	D3	57.00	27.00	29.41	1375	7.74	5.90
C	F1D1	D1	55.40	36.50	30.00	1246	6.12	4.19
	F2D2	D2	74.40	40.20	32.04	1657	9.42	5.45

3.2 Energy Dissipation

Toughness can be defined as the material's ability to deform plastically and absorb energy without fracturing. It can be obtained by calculating the area under the load-deflection curve. Depending on the experimental test results, the toughness of the specimens NCS with reinforcement details D2 and D3 increased by (65 and 84) %, respectively, compared to that of the reference specimens with conventional reinforcement detail D1. Also, the absorbed energy of high-strength specimens is increased when the reinforcement details D2 and D3 are used. The increasing ratio is (36 and 59) % for the specimens with reinforcement details D2 and D3, respectively. An increase of 33% has been achieved for the steel fiber reinforced concrete specimen with reinforcement steel detail D2 compared to conventional reinforcement detail D1 of the same concrete grade.

On the other hand, the amount of absorbed energy for the tested specimens increased when the concrete compressive strength increased. The energy absorption for high strength and steel fiber specimens compared with normal concrete with the same reinforcement steel details D1 increases by (42 and 105) %, respectively. An increase of (17 and 65) % was achieved by the specimens of reinforcement details D2 for both high strength and steel fiber reinforced concrete, respectively, more than the normal concrete with the same reinforcement detail. Also, the specimen of high strength concrete with reinforcement detail D3 appeared to increase the amount of absorbed energy by 23% more than the normal concrete specimen with the same reinforcement detail. The absorbed energy at the beam-column joint or any RC member equals the sum of absorbed energy by concrete and steel. When the concrete compressive strength increases or when additional internal steel for confining the concrete is used, the load capacity increases too, which means more energy is needed to make the specimen reaches the failure and the reinforcement reach the yield.

3.3 Ductility Index

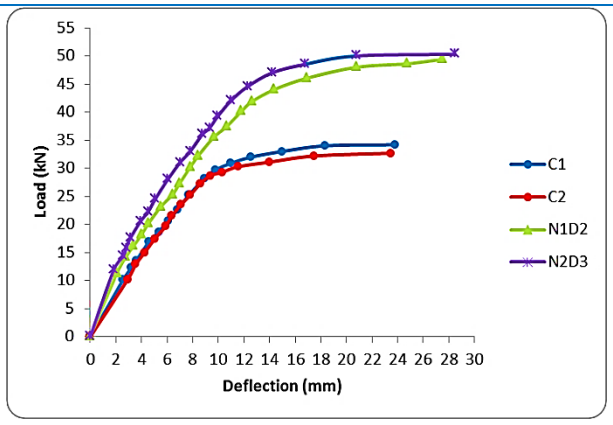
The material's ductility represents its ability to sustain deformation after its initial yield deformation while carrying the load. The ductility index can be obtained from the maximum deflection ratio to the yield deflection. Using internal closed stirrups and steel bars to confining the concrete increased the concrete compressive strength. Using steel fiber enhanced the ductility index for the tested specimen, as shown in Table (5). The (D.I) of the specimens of NSC that have reinforcement details D2 and D3 were increased by (16 and 23) % more than the reference specimens with reinforcement detail D1. An increase of the (D.I) for the specimens of HSC with reinforcement details D2 and D3 by (27 and 47) % compared to their normal reinforcement control specimen. The specimen of reinforcement detail D2 in the third

group of steel fiber reinforced concrete recorded an increase of 54% for its (D.I) with respect to the control specimen with conventional reinforcement detail D1.

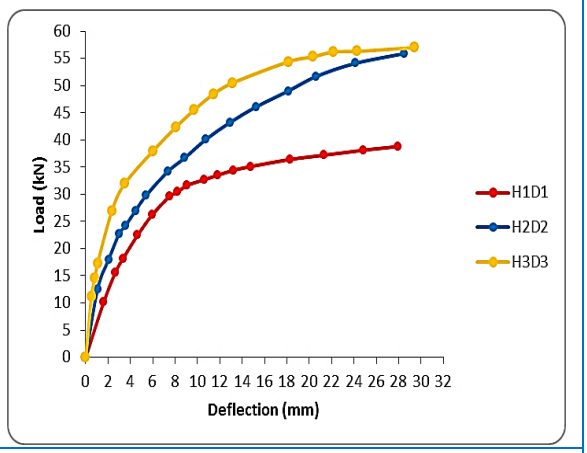
Moreover, the (D.I) is affected by using the steel fiber (2%) in steel fiber reinforced concrete. Where the steel fiber increases the tensile strength of the concrete and controls the cracks, and increases the cracking load. So, a significant increase for the specimens of SFRC by (124 and 198) % for the specimens with reinforcement details D1 and D2, respectively, compared to the normal concrete specimens with same reinforcement details.

3.4 Load–Deflection Response

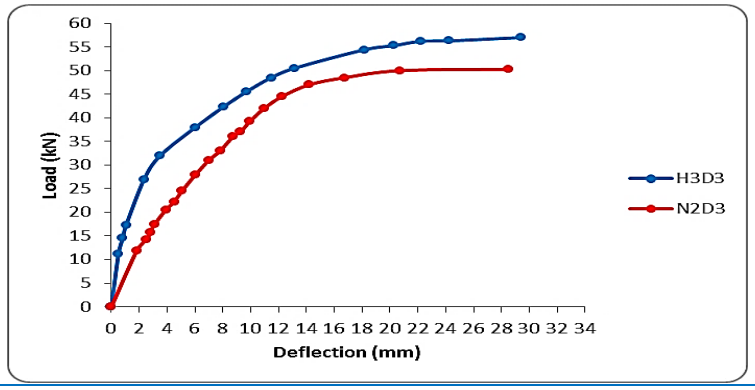
Figure 4 represents the curves of the load against mid-span deflection for each group separately. While Fig. 5 shows the load-deflection curves for each reinforcement detail D1, D2, and D3. From these curves, it is observed that the specimens of SFRC have maximum deflection compared to the specimens of HSC and NSC. That is due to the use of steel fiber, which leads to an increase in the ductility of concrete and increase in load-carrying capacity. Forever, the deflection of the specimens with reinforcement detail D2 and D3 are higher than of detail D1 due to the confining of concrete using internal additional steel bars and closed spacing stirrups. The additional internal closed stirrups and longitudinal steel bars arranged around the longitudinal axis of the specimen lead to improve the flexural and shear strength of the specimens. So, the specimen exhibits more bending and ductility than the control join.



(a) Load-deflection curve of NSC



(b) Load-deflection curve of HSC



(c) Load-deflection curve of SFRC

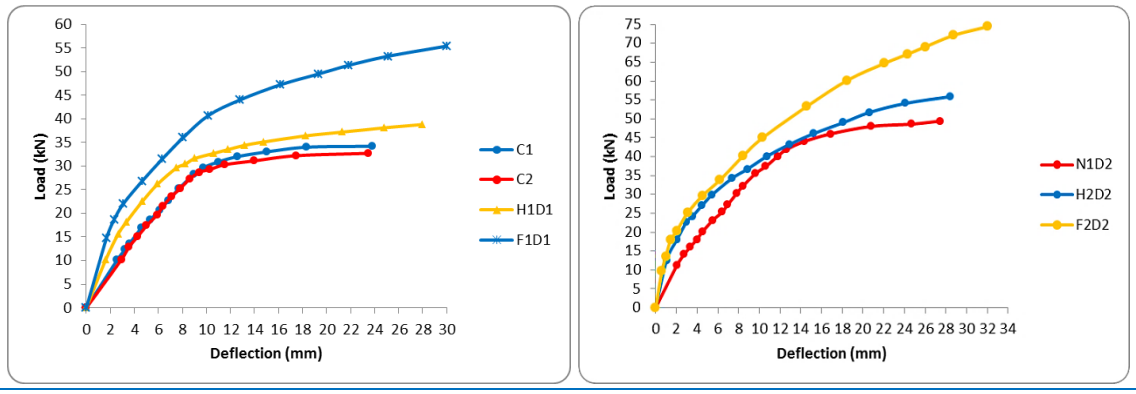
Fig. 4 Load – deflection curves corresponding to reinforcement details

3.5 Initial Stiffness

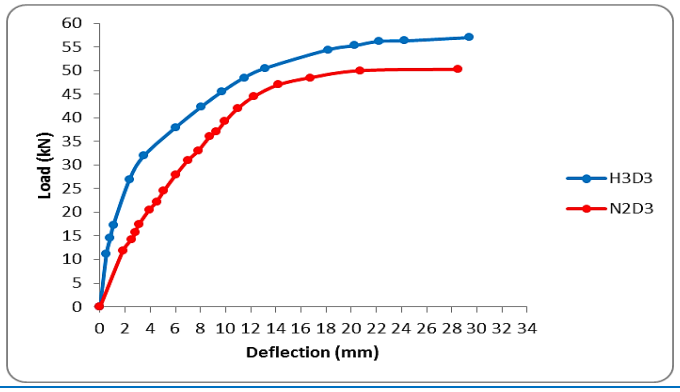
The Initial stiffness is obtained depending on the relation of the load-mid span deflection. It is equal to the slope of the drawn line passing through a point that lies on the load-deflection curve opposite to (70%) of the ultimate applied load. This line is extended to meet a horizontal line passing through a point that represents the ultimate load [19]. So,

$$InitialStiffness = \frac{P_u}{D_y} \quad (1)$$

Based on the results obtained from the experiment investigation and the load-deflection curves shown in Figures (4) and (5), It was observed that the initial stiffness of NSC specimens with reinforcement details D2 and D3 was higher than the control specimens with normal reinforcement detail by (11 and 21)%, respectively. In the HSC group, the initial stiffness of the specimens with reinforcement details D2 and D3 increased by (13 and 54) % compared to the reference specimen with normal internal details. While for SFRC, the specimen with internal detail D2 had an initial stiffness higher than the control by 30 %. Also, the concrete compressive strength affected the initial stiffness. The results of the specimens of the three groups (NSC, HSC, and SFRC) with the same reinforcement details that showed in Table (5) cleared that the SFRC specimen had got higher initial stiffness than other groups due to using of steel fiber where the initial stiffness increased by (27 and 49)% for the specimen with reinforcement details D1 and D2 respectively compared to the normal concrete specimens with same reinforcement details.



(a) Load-deflection curve of D1 (b) Load-deflection curve of D2



(c) Load-deflection curve of D3

Fig. 5 Load–deflection curves corresponding to compressive strength

3.6 Modes of Failure

The overall cracks patterns that have been observed in this investigation are flexural cracks. Several cracks began to appear almost at the middle distance of the beam length as micro-cracks. These cracks formed firstly due to different loads corresponding to the type of concrete, reinforcement detail, and strengthening or retrofitting techniques. They have been derived from the extreme fiber of the tension zone and took a vertical direction toward the compression region. Then, these cracks increased and expanded in addition to developing other cracks with the increase in the applied load to the tested specimen. The specimens' main cracks with reinforcement detail D2 and D3 are formed approximately at the edge of the additional internal reinforcement. Moreover, the number of cracks is increased with further increasing load. Fig.6 shows the crack pattern of all tested specimens.



(1) Crack Patterns of F1D1



(2) Crack Patterns of F2D2

(a) Crack patterns of steel fiber reinforced concrete specimens



(1) Crack Patterns of H1D1



(2) Crack Patterns of H2D2



(3) Crack Patterns of H3D3

(b) Crack patterns of high strength concrete specimens



(1) Crack Patterns of C1



(2) Crack Patterns of C2



(1) Crack Patterns of N1D2



(1) Crack Patterns of N2D3

(C) Crack patterns of normal strength concrete specimens

Fig .6 Crack patterns of RC Specimens according to a concrete type

4. Conclusions

From the results that have been obtained from the experimental work, the following conclusions can be drawn:

1. The control specimens contain conventical reinforcement details that exhibited sufficient strength, lower ductility, lower stiffness, and hence lower energy absorption compared with the specimens reinforced with a new style.
2. The load-carrying capacities of the tested specimens were improved by a range of (34 to 50) % due to confining of concrete using additional internal reinforcement steel bars and closed stirrups, i.e. (D2 and D3) led to an increase in the mid-span deflection of the specimens due to increasing of the steel ratio which improves the concrete tensile strength and increases the ductility characteristics of the specimens.
3. Increasing the concrete compressive strength by using high strength or steel fiber concrete led to an increase in the load-carrying capacity for the tested specimens with (13 to 66) %.
4. Confining concrete using internal steel bars and closed stirrups led to an increase in the ductility index.
5. The proposed details of reinforcements can be considered successful under static load. Hence, the investigations may be extended under different loading regimes such as cyclic or repeated load.

Acknowledgments

The researcher would like to thank and express the deepest gratitude grateful to everyone of construction labrotary at Al Amarah Technical Institute.

Author Contributions: The authors contributed to all parts of the current study.

Funding: This study received no external funding.

Conflicts of Interest: The authors declare no conflict of interest.

References

[1] Karayannis C. G., Chalioris C. E. and Sirkelis G. M. (2008), "Local retrofit of exterior RC beam-column joints using thin RC jackets—an experimental study", *Earthquake Engineering and Structural Dynamics*, **37**(5), 727-746.

[2] Ha, G. J. and Cho C. G. (2008), "Strengthening of reinforced high-strength concrete beam-column joints using advanced reinforcement details," *Magazine of concrete research*, **60**(7), 487-497.

[3] Le-Trung K., Lee K., Lee J., Lee D. H. and Woo, S. (2010), "Experimental study of RC beam-column joints strengthened using CFRP composites," *Composites Part B: Engineering*, **41**(1), 76-85.

[4] Mady M., El-Ragaby A. and El-Salakawy E. (2011), "Seismic behavior of beam-column joints reinforced with GFRP bars and stirrups," Journal of Composites for Construction, **15**(6), 875-886.

[5] Misir I. and Kahraman S. (2013), "Strengthening of non-seismically detailed reinforced concrete beam-column joints using SIFCON blocks," *Sadhana*, **38**(1), 69-88.

[6] Kannan P., Sivakumar S.and Bindhu, K. (2013), "Seismic strengthening of exterior RC beam-column joints by advanced ferrocement jacketing," *Int. J. Innovat. Res. Sci., Eng. Tech*, **2**(1), 53-58.
[7] Hadi M. N. and Tran T. (2014), "Seismic strengthening of exterior RC beam-column connections using concrete covers and CFRP."
[8] Chidambaram R. S. and Agarwal P. (2015), "Seismic behavior of hybrid fiber reinforced cementitious composite beam-column joints," Materials and Design, 86, 771-781.
[9] Bindhu K., Mohana N. and Sivakumar S. (2016), "New reinforcement detailing for concrete jacketing of nonductile exterior beam-column joints," *Journal of Performance of Constructed Facilities*, **30**(1), 04014192.
[10] De Risi M. T. Ricci P., Verderame G. M. and Manfredi G. (2016), "Experimental assessment of unreinforced exterior beam-column joints with deformed bars," *Engineering Structures*, **112**, 215-232.
[11] Balaji S. and Thirugnanam G. (2017), "Study on exterior RC beam-column joints upgrade with SIFCON in the joint core under reversed cyclic loading", *KSCE Journal of Civil Engineering*, **21**(1), 346-352.
[12] Torabi A. and Maheri M. R. (2017), "Seismic repair and retrofit of RC beam-column joints using stiffened steel plates," *Iranian Journal of Science and Technology, Transactions of Civil Engineering*, **41**(1), 13-26.
[13] Gokdemir H. and Tankut T. (2018), "Seismic strengthening of beam-column joints using diagonal steel bars," *Teknik Dergi*, **28**(ek), 2117-2130.
[14] Mostofinejad D. and Hajrasouliha M. (2018), "Shear retrofitting of corner 3D-reinforced concrete beam-column joints using externally bonded CFRP reinforcement on grooves", *Journal of Composites for Construction*, **22**(5), 04018037.
[15] Das P. and Choudhury S. (2018), "Experimental study on a fiber-reinforced concrete beam-column joint with ductile detailing under reversed cyclic loading," *International Journal of Engineering and Technology*, **7**(3.16), 85-89.
[16] Montava I., Irles R., Pomares J. C. and Gonzalez A. (2019), "Experimental study of steel-reinforced concrete (SRC) joints," *Applied Sciences*, **9**(8), 1528.
[17] Arowojolu O., Ibrahim A., Rahman M. K., Al-Osta M. and Al-Gadhib A. H. (2019), "Plastic hinge relocation in the reinforced concrete beam-column joint using carbon fiber–reinforced polymer," *Advances in Structural Engineering*, **22**(14), 2951-2965.
[18] Oinam R. M., Kumar P. and Sahoo D. R. (2019), "Cyclic performance of steel fiber-reinforced concrete exterior beam-column joints", *Earthquakes and Structures*, **16**(5), 533-546.
[19] Abdulraheem M. S. (2018), "Experimental investigation of fire effects on ductility and stiffness of reinforced reactive powder concrete columns under axial compression," *Journal of Building Engineering*, **20**, 750-761.